Emergent simplicity despite local complexity in eroding fluvial landscapes

Gareth G. Roberts

Department of Earth Science and Engineering, Imperial College London, UK

E-mail: gareth.roberts@imperial.ac.uk.

ABSTRACT

Much understanding of continental topographic evolution is rooted in measuring and predicting rates at which rivers erode. Flume tank and field observations indicate that stochasticity and local conditions play important roles in determining rates at small scales (e.g. < 10 km, thousands of years). Obversely, preserved river profiles and common shapes of rivers atop uplifting topography indicate that erosion rates are predictable at larger scales. These observations indicate that the response of rivers to forcing can be scale dependent. Here I demonstrate that erosional thresholds can provide an explanation for why profile evolution can be very complicated and unique at small scales yet simple and predictable at large scales.

INTRODUCTION

Landscape evolution is a response to physical, chemical and biologic processes operating across a broad range of scales (e.g. Gasparini et al. 2006, Anderson & Anderson 2010, Egholm et al. 2013). Conversely, it plays an important role in determining geologic, chemical, climatic and biologic evolution, and in distributing natural resources (e.g. Howard et al. 1994, Scheingross et al. 2019, Fernandes et al. 2019). I focus on physical erosion of longitudinal river profiles carved into bedrock, which can set the pace of landscape evolution in low to mid-latitudes (e.g. Young & McDougall 1993, Rosenbloom & Anderson 1994, Howard et al.

1994, Sklar & Dietrich 1998, Whipple & Tucker 1999, 2002).

Many natural systems, including rivers are characterized by scale dependent complexity (e.g. Roberts et al. 2019). At small scales, e.g. < O(10) km, < O(10^3) years, erosion rates (and river profile evolution) can be highly variable and dynamical physics-based models have been developed to understand observed complexity (e.g. Lamb et al. 2008). At larger scales river profile evolution is often explored using phenomenological (essentially kinematic) models that capture emergent simplicity (e.g. stream power model; Rosenbloom & Anderson, 1994). Preliminary work examining the spectral content of river profiles suggests that their geometries are scale dependent (e.g. Roberts et al. 2019; Wapenhans et al., 2021). These observations suggest that different physical processes control river profile evolution at the diverse scales of interest (up to O(10^3) km).

Here, I seek an understanding of how scale dependent river geometries emerge and, relatedly, how physics-based erosional models and insights from phenomenological approaches might be formally reconciled. I test three hypotheses. First, most erosional processes can be described using simple threshold models. Secondly, erosional thresholds are responsible for generating complexity at small scales and emergent simplicity. Finally, simple threshold models can replicate predictions of phenomenological (e.g. stream power) models. The approach taken here is akin to particle-based landscape evolution modeling (e.g. Lamb et al. 2008, Tucker & Bradley 2010).

PRELIMINARY WORK

River profile evolution is often predicted using relatively simple kinematic models, which can yield low residual misfits to observed profiles, despite not explicitly considering processes

50 that determine erosion rates at some scales (e.g. hydrodynamics, substrate changes; Sklar
51 & Dietrich 1998, Tinkler & Wohl 1998, Stock & Montgomery 1999, Lamb & Dietrich 2009,
52 Roberts & White 2010, Salles 2016, Fernandes et al. 2019, Glade et al. 2019, Scheingross
53 et al. 2019). One example is the stream power model, which can be expressed as
54
55 $$\frac{\partial z}{\partial t} = -vA^m \left|\frac{\partial z}{\partial x}\right|^n + U(x,t) + \eta(x,t). \quad [1]$$
56

57 In this scheme, which is usually presented without accompanying noise (η), erosion rate is
58 set by the velocity of kinematic erosional 'waves' that propagate upstream. The rate at which
59 slopes, ∂z/∂x, propagate is set by the erosional prefactor v, upstream drainage area, A(x),
60 and exponent m as a proxy for discharge. If n ≠ 1 propagating slopes can induce shocks
61 (e.g. steeper slopes can overtake gentler slopes; see Pritchard et al. 2009). Elevation, z, is
62 typically added to profiles by assuming the form of uplift rate, U, which can vary as a function
63 of space, x, and time, t. Examples of solutions to Equation 1 are shown in Figure 1a-c. The
64 black curves in Figure 1a show river profile evolution calculated by solving Equation 1
65 (Roberts & White 2010). For simplicity, in this example n = 1, v = 2 km /Ma, m = 0 (i.e.
66 advective velocities are constant). Figure 1b shows calculated river profiles colored by age.
67 Calculated incision is shown in Figure 1c. The gray curves in Figure 1a and 1c show results
68 for additional monotonic noise (η > 0), which generates a few meters of relief. These results
69 indicate that long wavelength structure can emerge through local complexity in simple
70 phenomenological models of landscape evolution (Roberts et al. 2019). The theory of
71 stochastic partial differential equations gives a basis for understanding why some natural
72 phenomena generate relatively simple structures at large scales despite considerable local
73 complexity (Kardar et al. 1986, Hairer 2014). Pioneering geomorphic work has also related
74 erosional processes operating at small scales to larger-scale landscape evolution (Smith &

Bretherton 1972, Birnir et al. 2001, see also Dodds et al. 2000, Rinaldo et al. 2014).

NEW METHODS

I seek an explanation for why 'simple' landscape forms and erosional histories should emerge despite myriad local complexities. As a starting point, an erosional threshold model is used to examine whether scale dependent complexity can emerge from local erosional processes. This simple model has three advantages. First, it can be straightforwardly related to physics-based models (see Supplementary Material). Second, it is probably a reasonably universal description for how rivers erode at small scales. Finally, its simplicity means that it is trivial to estimate statistical properties by brute force (i.e. by running many models with random starting conditions).

A variety of physics-based models could be used to explore evolution of river profiles. Models might, for example, include the cohesive strength of rock, alluvial cover especially where slopes are low, or the Shields parameter (Supplementary Material). In this paper, thresholds for erosion to occur, c, are set to be the local relief (height, Δz) that must be exceeded (i.e. erosion occurs if $\Delta z > c$). This simple measurable quantity can be easily compared to independent observations. It can also be straightforwardly related to models of block toppling, which appear to set the rate of erosion in some settings (e.g. Lamb & Dietrich 2008, Stucky de Quay et al. 2019). Such models relate stability of rock columns to water discharge via torque (moment) calculations. For example, ideal blocks of rock partially submerged in water subject to shear stresses along their upper surfaces and drag on surfaces facing upstream will remain stable if,

$$\frac{\frac{1}{2}L(F_g - F_b)}{F_d(H - h_1/2) + F_\tau H} \geq 1 \quad [2]$$

where L is the width of the column, and F_g, F_b, F_d and F_τ are forces related to mass of the rock column, buoyancy, drag and shear. H is the height of the rock column and h_1 is the length over which drag acts upon the exposed part of the column (see Supplementary Material). Surface and body forces depend on densities of water and rock, water discharge, gravitational acceleration and the geometric properties of the landscape (e.g. slopes). Most are measurable at the present-day and reasonable bounds can be estimated a short way back in time (e.g. from gauge station data). This simple scheme can be simplified further if we assume that blocks will topple if their height exceeds a critical value, c, which could be expressed as a function of, for example, F_g, F_b, F_d, F_τ (Supplementary Material). In this scheme, which is cast in terms of position along a river, x, and time, t, elevation, z, becomes

$$z_{t+1}^x = \begin{cases} z_t^x & if \ \Delta z \leq c, \\ z_t^x - \Delta z & if \ \Delta z > c, \end{cases} \quad [3]$$

where $\Delta z = z_t^x - z_t^{x-1}$. This model requires a starting condition, i.e. z(x) at t = 0. In the first test, a random uniform distribution of elevations is generated and then ordered by height such that the starting condition is monotonic (Figure 1d-i). This starting condition is then evolved by solving Equation 3. Different starting and threshold conditions are also tested including white noise, concave- and convex-upward profiles and c(x,t). Movies in Supplementary Information show the time dependent behavior of the model.

RESULTS AND DISCUSSION

Solving Equation 3 using a random, monotonic distribution of elevations as the starting

condition, and a constant value of c that is a few percent of maximum local relief, is shown in Figure 1d-g. The same results are shown at larger scales in Figure 1h-i. This simple model generates three insights. First, because tall blocks ($\Delta z > c$) topple and short blocks ($\Delta z < c$) do not, steeper slopes propagate faster than gentler slopes at the reach scale (Figure 1d–g). This effect results in steeper sections of the river cannibalizing less steep sections. This kinematic behavior is a manifestation of shockwaves. Second, propagating blocks quickly reach a stable height, which is proportional to c, but also depends on the initial distribution of elevations. These geometric properties appear to determine the emergence of simplicity at large scales. The number of blocks moving through time decreases by a few percent in a stepwise fashion (Supplementary Material). At larger length and timescales, the system is more stable (Figure 1h–i), and the propagation rate of slopes upstream approaches linearity (i.e. there are no more shocks; Supplementary Movie 1). This set of results suggests that simple physics-based models of fluvial erosion can predict highly non-linear, complex and cannibalizing behavior at small scales and emergent, simple, linearly evolving profiles at larger scales. To achieve similar behavior with a stream power erosional model would require slope exponent $n \neq 1$ at small scales and $n = 1$ at larger scales (e.g. Pritchard et al. 2009; Lague 2014).

Figure 2 shows results for block toppling models with different starting conditions. The first example mimics the model already examined in Figure 1d-i but, in this case, a random uniform distribution of (white) noise was added to a simple linear profile (i.e. slopes can be locally positive or negative; see Supplementary Material). The results from this model generate essentially the same long wavelength behavior as the example with monotonic changes in elevation (Figure 1d-i). The time dependent behavior of this threshold model is compared to predictions from the stream power model (Equation 1 with $\eta = 0$) in Figure 1b.

149 The threshold c is constant in the block toppling model and the stream power model has the
150 following Dirichlet boundary conditions: at the head $z = z_o$ where z_o is elevation of the starting
151 solution, and z = 0 at the mouth. The results indicate that the stream power and threshold
152 models generate very similar predictions of long wavelength longitudinal profile evolution.
153 An example of an evolving concave-upward profile is shown in Figure 1c-d. The block
154 toppling model has the same distribution of added noise and critical height, c, as for the
155 model shown in Figure 2a, and the boundary conditions for the stream power model are the
156 same. This experiment was performed to examine evolution of profiles that might once have
157 been at steady state (i.e. dz/dt = 0, U = E; Figure 2c). Finally, evolution of a profile that
158 contains a large knickzone, which might have been generated by, say, a spatially uniform
159 change in uplift rate, is examined in Figure 2e-f. As expected, the stream power model
160 'smears' profile evolution close to the lower boundary condition. In all cases examined the
161 stream power model predicts very similar profile evolution to the simple physical model at
162 large scales. The evolution of these profiles show that long wavelength simplicity can
163 emerge despite locally complex erosion. Unsurprisingly, changing the distribution of c
164 affects the evolution of theoretical rivers. For example, increasing or decreasing c means
165 that fewer or more blocks migrate, respectively. If c varies in space and time simplicity can
166 also emerge (Supplementary Material). If c is larger than a few percent of local relief in the
167 starting condition river profile evolution begins to resemble staircases at large scales in
168 these examples with uniform distributions of noise.
169
170 The threshold model makes other predictions that might be fruitful avenues for further work.
171 They include autogenic growth of waterfalls, waterfall spacing and height, and fluvial
172 terraces at the crest of waterfalls that are curved as shocks propagate but flat along their
173 base. An initial assessment suggests that these predictions are consistent with some

geomorphic observations (e.g. Stucky de Quay et al. 2019, Scheingross et al. 2020; Figure 1g).

CONCLUSIONS

The simple threshold models examined predict slopes that can propagate at different velocities at short length and time scales such that steeper slopes can overtake (and cannibalize) gentler slopes. At longer time scales the model retains local complexity (e.g. changes in slope at a range of length scales). In the examples examined, these local changes in relief are nested within longer wavelength slopes that propagate upstream in a predictable way (e.g. Figure 1g-i). This emergent simplicity gives support for the use of phenomenological models (e.g. stream power) to predict river profile evolution at large scales (e.g. Figure 2b, c, f). The models explored in this paper are somewhat arbitrary and further work could explore conditions under which complexity at small scales does not lead to emergent simplicity. In summary, simple physics-based models of fluvial erosion that include thresholds can predict local complexity and naturally emergent simplicity at larger scales.

Acknowledgments

A. Bufe, V. Fernandes, A. Lipp, C. O'Malley, F. Richards, J. Scheingross, G. Stucky de Quay, N. White and A. Wickert are thanked for their help. This work was supported by the Leverhulme Trust (RPG-2019-073).

Figure 1. Fluvial erosion at large scales from stream power model (a-c), and scale dependent river profile evolution from simple physics-based models (d-i). (a) Black/gray curves = longitudinal river profiles at 0–23 Ma calculated by solving the stream

power model with no/small noise. (b) River profile evolution for stream power model with a small amount of noise, colored with linear scale to 5 Ma. (c) Incision as a function of time for profiles shown in panel (a); gray/black = noisy/noiseless models. (d) Reach scale: River profile (white blocks; elevation as a function of distance) at time, t = 0. Critical relief (c, for toppling) is shown inset. Gray = air/water. (e–g) River profile evolution as a function of time calculated by solving Equation 3. Note that older river profiles are shown by lighter colors; profiles propagate upstream (towards left of these panels). (h) Zooming out by order of magnitude; white box = panel g. (i) Zooming out by a further factor of ~ 3, white box = panel h. Note color scale has been linearly scaled to show river profile evolution between $0 \leq t \leq 100$. Note emergence of linear slope propagation at large length and time scales.

Figure 2. Comparison of predicted river profile shapes from stream power and block toppling models. (a) Solutions to threshold (block toppling model; Equation 3) for a single long wavelength slope with added uniform distribution of noise. Evolution during first 100 timesteps is shown by rainbow color scheme; light gray curves = profile every 100 timesteps, increasing in age to the left. (b) Gray = profiles predicted by threshold model at 0, 100, 200 and 300 (t_0-t_3) time steps. Black = predictions from stream power model. The stream power models shown in this figure are forced with constant v, n = 1, m = 0, U = η = 0, they have fixed (Dirichlet) boundary conditions (see Equation 1 and body text). (c-d) and (e-f) Predicted longitudinal river profiles from concave-upward (e.g. 'steady-state') and convex-upward starting conditions, respectively.

References

Anderson, R. S. & Anderson, S. P. (2010), Geomorphology: The mechanics and chemistry of landscapes, Cambridge University Press.

Birnir, B., Smith, T. R. & Merchant, G. E. (2001), 'The scaling of fluvial landscapes', Computers & Geosciences 27(10), 1189–1216.

Dodds, P. S. & Rothman, D. H. (2000), 'Scaling, Universality, and Geomorphology', Annual Review of Earth and Planetary Sciences 28(1), 571–610.

Egholm, D., Knudsen, M. & Sandiford, M. (2013), 'Lifespan of mountain ranges scaled by feedbacks between landsliding and erosion by rivers', Nature 498, 475–478.

Fernandes, V. M., Roberts, G. G., White, N. & Whittaker, A. C. (2019), 'Continental-Scale Landscape Evolution: A History of North American Topography', Journal of Geophysical Research: Earth Surface 124, 1–34.

Gasparini, N. M., Bras, R. L., Whipple, K. X. (2006), 'Numerical modeling of non-steady-state river profile evolution using a sediment-flux-dependent incision model', GSA Spec. Pap. 398, doi:10.1130/2006.2398(08).

Glade, R. C., Shobe, C. M., Anderson, R. S. & Tucker, G. E. (2019), 'Canyon shape and erosion dynamics governed by channel-hillslope feedbacks', Geology 47(7), 650–654.

250 Hairer, M. (2014), ‘A theory of regularity structures’, Invent. math. 198, 269–504.
251
252 Howard, A. D., Dietrich, W. E. & Seidl, M. A. (1994), ‘Modeling fluvial erosion on regional to
253 continental scales’, Journal of Geophysical Research: Solid Earth 99(B7), 13971– 13986.
254
255 Kardar, M., Parisi, G. & Zhang, Y.-C. (1986), ‘Dynamic Scaling of Growing Interfaces’, Phys.
256 Rev. Lett. 56, 889–892.
257
258 Lague, D. (2014), ‘The stream power river incision model: evidence, theory and beyond’,
259 Earth Surface Processes and Landforms 39, 38–61.
260
261 Lamb, M. P. & Dietrich, W. E. (2009), ‘The persistence of waterfalls in fractured rock’,
262 Geological Society of America Bulletin 121(7-8), 1123–1134.
263
264 Pritchard, D., Roberts, G., White, N. & Richardson, C. (2009), ‘Uplift histories from river
265 profiles’, Geophysical Research Letters 36(24).
266
267 Rinaldo, A., Rigon, R., Banavar, J. R., Maritan, A. & Rodriguez-Iturbe, I. (2014), ‘Evolution
268 and selection of river networks: Statics, dynamics, and complexity’, Proceedings of the
269 National Academy of Sciences 111(7), 2417–2424.
270
271 Roberts, G. G. (2019), ‘Scales of Similarity and Disparity Between Drainage Networks’,
272 Geophysical Research Letters 46(7), 3781–3790.
273
274 Roberts, G. G. & White, N. (2010), ‘Estimating uplift rate histories from river profiles using

275 African examples', Journal of Geophysical Research: Solid Earth 115(B2).
276
277 Roberts, G. G., White, N., Lodhia, B. H. (2019), 'The generation and scaling of longitudinal
278 river profiles', Journal of Geophysical Research: Earth Surface, doi:10.1029/2018JF004796.
279
280 Rosenbloom, N. A. & Anderson, R. S. (1994), 'Hillslope and channel evolution in a marine
281 terraced landscape, Santa Cruz, California', Journal of Geophysical Research: Solid Earth
282 99(B7), 14013–14029.
283
284 Salles, T. (2016), 'Badlands: A parallel basin and landscape dynamics model', SoftwareX 5,
285 195–202. URL: http://linkinghub.elsevier.com/retrieve/pii/S2352711016300279
286
287 Scheingross, J. S., Lamb, M. P. & Fuller, B. M. (2019), 'Self-formed bedrock waterfalls',
288 Nature 567, 229–233.
289
290 Scheingross, J. S., Limaye, A. B., McCoy, S. W., Whittaker, A. C. (2020), 'The shaping of
291 erosional landscapes by internal dynamics', Nature Reviews, doi:10.1038/s43017-020-
292 0096-0.
293
294 Sklar, L. & Dietrich, W. E. (1998), 'River longitudinal profiles and bedrock incision models:
295 Stream power and the influence of sediment supply', Geophysical Monograph - American
296 Geophysical Union 107, 237–260.
297
298 Smith, T. R. & Bretherton, F. P. (1972), 'Stability and the Conservation of Mass in Drainage
299 Basin Evolution', Water Resources Research 8(6), 1506–1529.

300

301 Stock, J. D. & Montgomery, D. R. (1999), 'Geologic constraints on bedrock river incision
302 using the stream power law', Journal of Geophysical Research: Solid Earth 104(B3), 4983–
303 4993.

304

305 Stucky de Quay, G., Roberts, G. G., Rood, D. H. & Fernandes, V. M. (2019), 'Holocene uplift
306 and rapid fluvial erosion of iceland: A record of post-glacial landscape evolution', Earth and
307 Planetary Science Letters 505, 118–130.

308

309 Tinkler, K. J. & Wohl, E. E. (1998), Rivers over rock: Fluvial Processes in bedrock channels.
310 Am. Geophys. Union Geophys. Mono. 107, 323pp.

311

312 Wapenhans, I., Fernandes, V. M., O'Malley, C., White, N. & Roberts, G. G. (2021), 'Scale-
313 Dependent Contributors to River Profile Geometry', Journal of Geophysical Research: Earth
314 Surface, doi:10.1029/2020JF005879.

315

316 Whipple, K. X. & Tucker, G. E. (1999), 'Dynamics of the stream-power river incision model:
317 Implications for height limits of mountain ranges, landscape response timescales, and
318 research needs', Journal of Geophysical Research: Solid Earth 104(B8), 17661– 17674.

319

320 Whipple, K. X. & Tucker, G. E. (2002), 'Implications of sediment-flux-dependent river incision
321 models for landscape evolution', Journal of Geophysical Research: Solid Earth 107(B2).

322

323 Wong, M & Parker, G. (2006), Re-analysis and correction of bedload relation of Meyer-Peter
324 and Muller using their own database, J. Hydraul. Eng., 132(11), 1159—1168.

Young, R. & McDougall, I. (1993), ‘Long-Term Landscape Evolution: Early Miocene 13 and Modern Rivers in Southern New South Wales, Australia’, The Journal of Geology 101(1), 35–49.

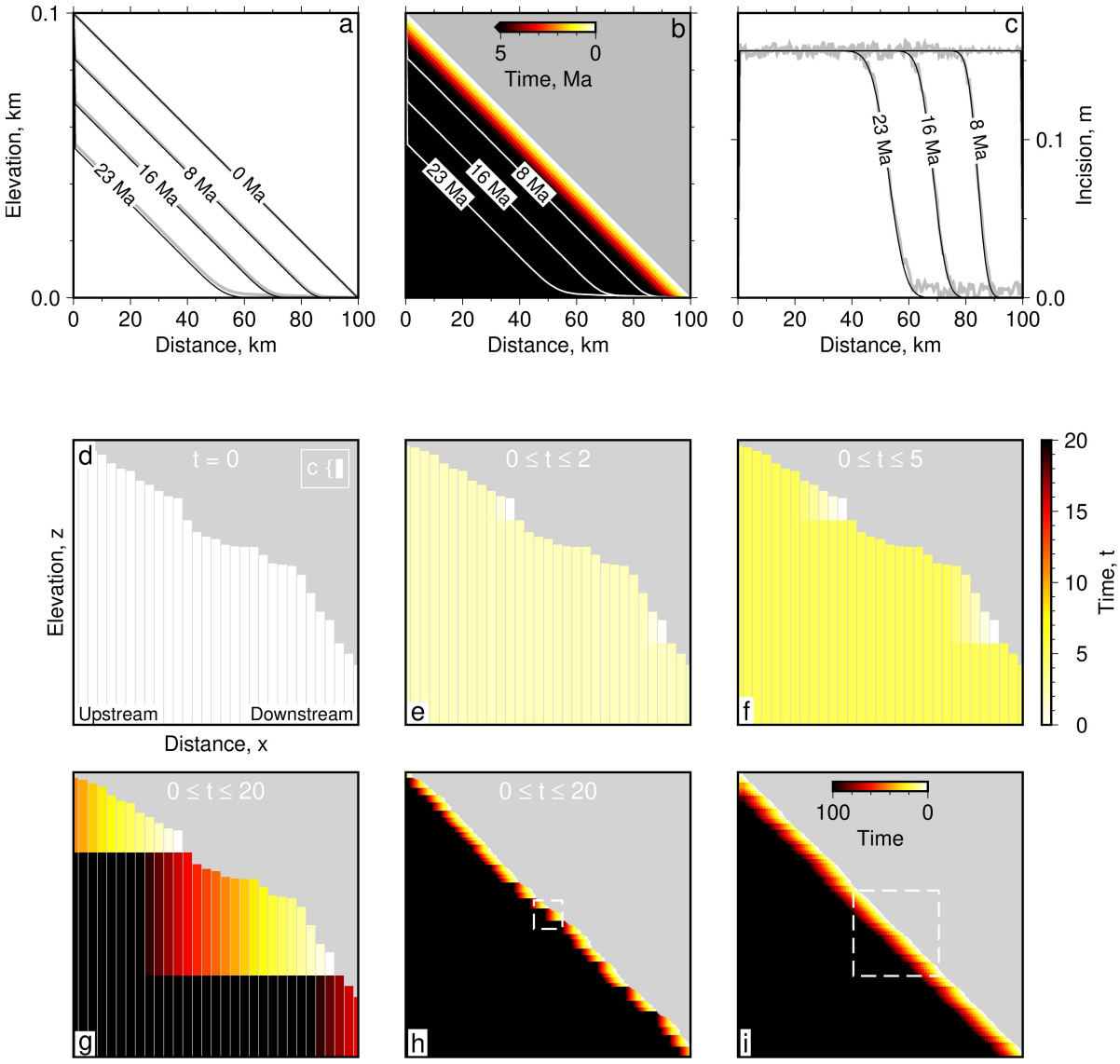

Figure 1

335

336

337

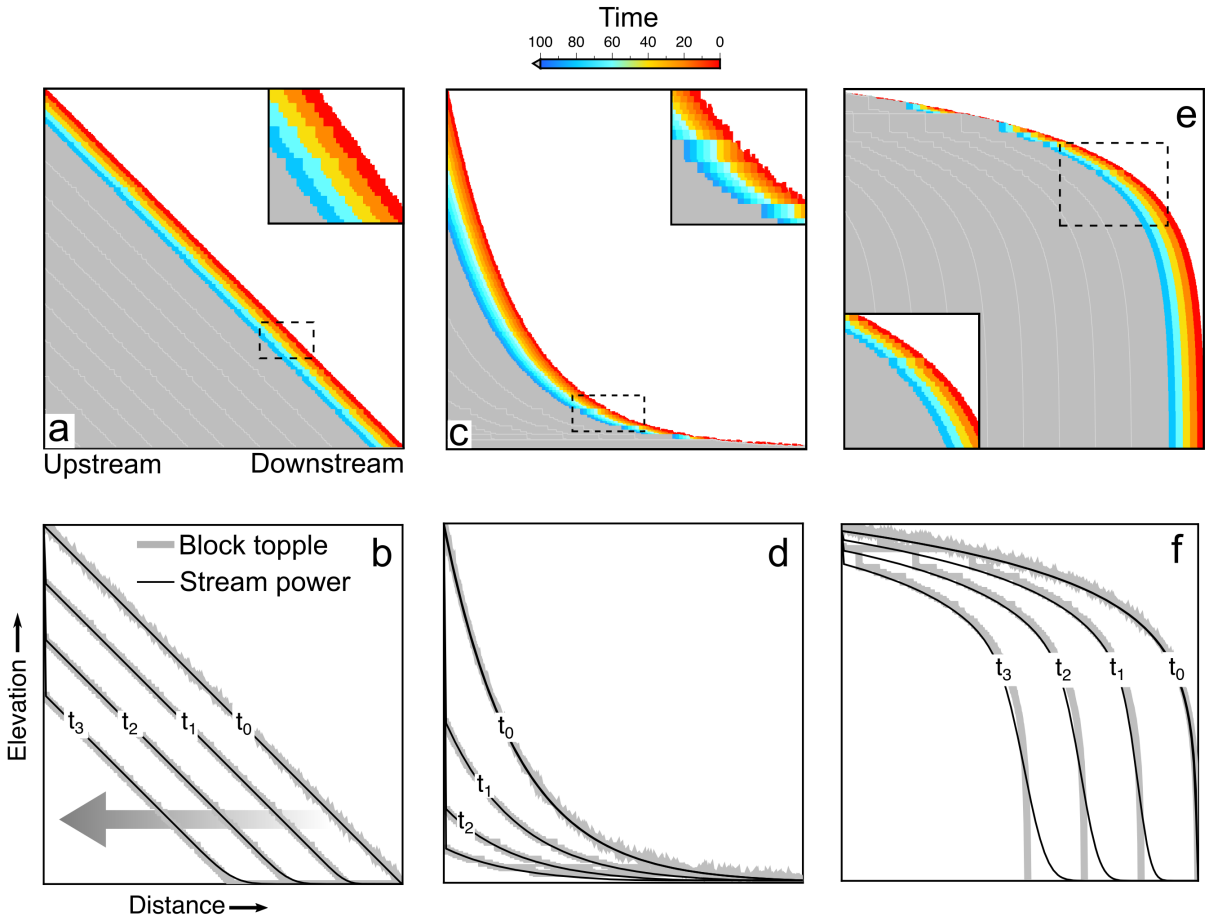

Figure 2

Supplementary Material for 'Emergent simplicity despite local complexity in eroding fluvial landscapes'

Gareth Roberts, gareth.roberts@imperial.ac.uk
Department of Earth Science and Engineering, Imperial College London, UK

Summary

This Supplementary Information contains two movies (details follow) and a simple mathematical explanation for how models of physical erosion can be simplified to very few parameters. The simple (few parameter) model is amenable to a straightforward, computationally inexpensive, exploration of parameter space at much larger scales. For example, Figure 2 shows the results of running the model where the evolution of 10^5 blocks is predicted for 10^5 time steps, which takes 50 s using a 2.6GHz Intel Core i7 processor. Finally, results showing the effect of changing the critical threshold value, c, are given in Figure 3 of this document. Results are described in the main manuscript and the movies help to show the time dependent behaviour.

Movies

Movie 1 shows the time dependent evolution of solutions to Equation (3) in the main manuscript for constant critical toppling height, c. The upper panel and inset show the evolution of the river coloured by timestep. The inset panel shows the region contained within the black box shown in the main panel. The rectangular panels below show relief along the river as a function of time, Δz, and relief greater than the critical value for toppling. The square panels below show frequency (black bars) and cumulative frequency (red curves) of relief. Solutions for the same model are also shown in Figure 1d-i of the main manuscript and as red solid and dotted curves in Figure 3b of this document. Movie 2 shows the distribution of relief generated by running this model 100 times with random (but uniformly distributed) starting conditions.

Simplifying a physical model of block toppling

The following describes how physical models of erosion along rivers can be described as a consequence of thresholds. The resultant simple models have very few parameters. In the main manuscript a simple (few parameter) model is explored for insights into the evolution of fluvial landscapes from very small (meter) to large (tens to hundreds of kilometres) scales.

Physical erosion is a consequence of body or surface forces (F) being sufficiently large that erosional thresholds, c, are exceeded. More formally, in discrete notation, at any position along a river, x, elevation will change as function of time, t, such that

$$z^x_{t+1} = \begin{cases} z^x_t & \text{if} \quad F \leq c \\ z^x_t - \Delta z & \text{if} \quad F > c, \end{cases} \tag{1}$$

where Δz is change in elevation, which can be set by, for example, the size of the rock mass (e.g. pebble, basalt column, fractured schist) being moved between time t and $t+1$. This simple description could be expanded to incorporate, for example, shear stresses or drag and critical thresholds for sliding, saltation, toppling or fracturing. The simple model appears to be a universal description of physical erosion along rivers. This supplementary document shows

one way in which a simple physical model of blocks toppling (e.g. Lamb & Dietrich, 2008; Stucky de Quay et al., 2019), which appears to be a reasonably description of fluvial erosion in regions of exposed bed rock, can be reduced to a simple model in which erosion occurs if rock column height exceeds a critical value for toppling (i.e. $\Delta z > c$). It is straightforward (and computationally efficient) to expand this model so that the consequences of local physical erosion for fluvial erosion at much larger scales can be explored. Simplification of other well known erosional models (wear; transport-limited erosion) are also examined.

In the simple scheme explored here, the propensity of columns of rock to topple is estimated as a function of drag, shear stress, rock mass and buoyancy. The force generated by drag on the (unit width) column of rock can be expressed as

$$F_d = \frac{1}{2}\rho_w C_d u^2 h_1, \tag{2}$$

where ρ_w is density of water, C_d is the dimensionless drag coefficient, u is water velocity, h_1 is height of the column exposed to flowing water. For reasonable values of parameters (see Table 1) in Equation (1), F_d is $\mathrm{O}(10^3 - 10^6)$ N for a column of unit width. The force generated by shear at the top of the unit width column can be expressed as

$$F_\tau \approx \rho_w g h_2 \frac{\mathrm{d}z}{\mathrm{d}x} L, \tag{3}$$

where g is gravitational acceleration, h_2 is depth of the flowing water, $\mathrm{d}z/\mathrm{d}x$ is channel bed slope, and L is width of the column. F_τ is expected to be $\mathrm{O}(10 - 10^3)$ N for slopes between $\mathrm{O}(10^{-3} - 10^{-2})$. The buoyancy force generated as a result of water displaced by the column of unit width rock can be expressed as

$$F_b = \rho_w g L h_3, \tag{4}$$

where h_3 is depth of the water at the base of the column. F_b is expected to be up to $O(10^5)$ N. The force exerted by the column of unit width rock is

$$F_g = \rho_r g L H, \tag{5}$$

where ρ_r is density of the rock column. F_g is expected to be up to $\mathrm{O}(10^5)$ N.

Calculating moments (see Figure 1) generated by application of these forces indicates that the column of rock will topple if

$$2HF_\tau + F_d\left(2H - h_1\right) + LF_b \geq LF_g. \tag{6}$$

Substituting Equation (4) into (6) and rearranging to make column height the subject yields

$$H\left[2F_\tau + 2F_d - L^2\rho_r g\right] \geq h_1 F_d - LF_b. \tag{7}$$

If $2F_\tau + 2F_d \geq L^2\rho_r g$, the column will topple if,

$$H \geq \frac{h_1 F_d - LF_b}{2F_\tau + 2F_d - L^2\rho_r g}. \tag{8}$$

If $2F_\tau + 2F_d < L^2\rho_r g$, the column will topple if,

$$H \leq \frac{h_1 F_d - LF_b}{2F_\tau + 2F_d - L^2\rho_r g}. \tag{9}$$

The right hand side of Equation (9) is less than unity for the parameter values given in Table 1. In other words blocks are likely to be stable if $2F_\tau + 2F_d < L^2\rho_r g$. We therefore focus on Equation (8). It is desirable to recast this equation in terms of elevation, z. For simplicity, if we assume that the right hand side of Equation (8) is constant, c, the evolution of longitudinal river profile elevations can then be expressed as

$$z_{t+1}^x = \begin{cases} z_t^x & \text{if} \quad \Delta z \leq c \\ z_t^x - \Delta z & \text{if} \quad \Delta z > c, \end{cases} \tag{10}$$

where $H = \Delta z$ (i.e. change in relief between adjacent columns; $\Delta z = z_t^x - z_t^{x-1}$), and x is position along the river. Solutions to Equation (10) are shown in the main manuscript and below for different starting conditions and distributions of c.

Examples of simplifying alternative erosional models

There are many ways in which river beds lower including by removal of alluvium or abrasion of bedrock. It seems likely that many erosional processes can be recast in a similar form to Equation (10). For example, if we consider erosion by wear, following Lamb et al. (2008)'s recasting of Cutter's (1960) classic impact wear model, the volume of bedrock eroded due to wear can be expressed as $V_i = V_p\rho_s w^2/2\epsilon$. V_p, ρ_s and w are the respective volume, density and impact velocity of particles (normal to the bed; e.g. saltating sediment). ϵ is the 'deformation wear factor', in other words the amount of energy required to remove a unit volume of eroded rock by wear, which incorporates the capacity of bedrock to store energy elastically. Note that, following Lamb et al. (2008), in this example there is no threshold kinetic energy for erosion to occur, except that the kinetic energy ($V_p\rho_s w^2/2$) must be greater than zero. For this simple scheme Equation (10) can be rewritten as

$$z_{t+1}^x = \begin{cases} z_t^x & \text{if} \quad V_p\rho_r w^2/2 \leq c \\ z_t^x - \Delta z & \text{if} \quad V_p\rho_r w^2/2 > c, \end{cases} \tag{11}$$

where c is 0 and Δz is V_i/A; A is the area of eroded bed rock removed. Clearly some of the scalings in this model are different to those considered in the block toppling model, however, the overarching rule (i.e. lowering occurs once a threshold has been exceeded) remains the same.

Perhaps more speculatively, if we consider transport-limited erosion, e.g. lowering of river profiles by movement of alluvium currently at rest, we can recast Equation (10) as

$$z_{t+1}^x = \begin{cases} z_t^x & \text{if} \quad \tau < c \\ z_t^x - \Delta z & \text{if} \quad \tau \geq c, \end{cases} \tag{12}$$

where $c = (\rho_r - \rho_w)gD$, i.e. we assume movement initiates at the Shields number, $\tau_* = \tau/c$. An important complexity is that Δz is likely to scale with shear stress and at short timescales it is expected to be a fraction of the diameter of the characteristic particle being moved, D (e.g. Wong & Parker, 2006).

All of these schemes can be made more complex (complete), for example, we might combine them, consider angular impingement of water or rock particles on bed rock, cohesive strength of joints, disentrainment of sediment, etc. It seems likely that in many models of physical erosion there is a critical threshold to overcome for erosion to initiate, which indicates that Equation (1) is perhaps a reasonable general representation of fluvial erosion.

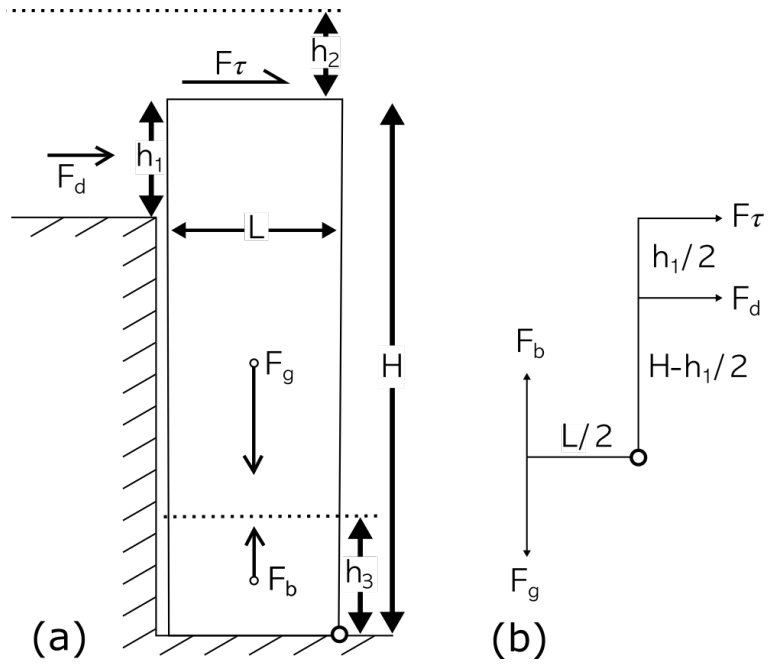

Figure 1: **Schematic block toppling.** (a) H and L = height and length of rock column. F_d = drag force on column exerted over length h_1. F_τ = shear force; h_2 = depth of water flowing across top of column. F_g = body force exerted by rock column. F_b = buoyancy force; h_3 = depth of displaced water at base of column. $\circ$ = pivot for moments calculations. (b) Schematic for torque calculation.

Table 1: Parameters and their values used for moments calculations.

Parameter	Notation	Value	Unit
Density of water	ρ_w	1	$\times 10^3$ kg m^{-3}
Drag coefficient	C_d	O(1)	Dimensionless
Velocity of water	u	O(1–10)	m s^{-1}
Height of column facing water	h_1	O(1–10)	m
Gravitational acceleration	g	9.81	m s^{-2}
Depth of flowing water	h_2	O(1–10)	m
Average slope	$\mathrm{d}z/\mathrm{d}x$	O($10^{-3} - 10^{-2}$)	Dimensionless
Width of rock column	L	O(1)	m
Displaced water	h_3	O(1–10)	m
Density of rock	ρ_r	2–3	$\times 10^3$ kg m^{-3}
Height of rock column	H	O(1–10)	m
Elevation	z	O(1–1000)	m
Change in elevation between adjacent columns	Δz	O(1–10)	m

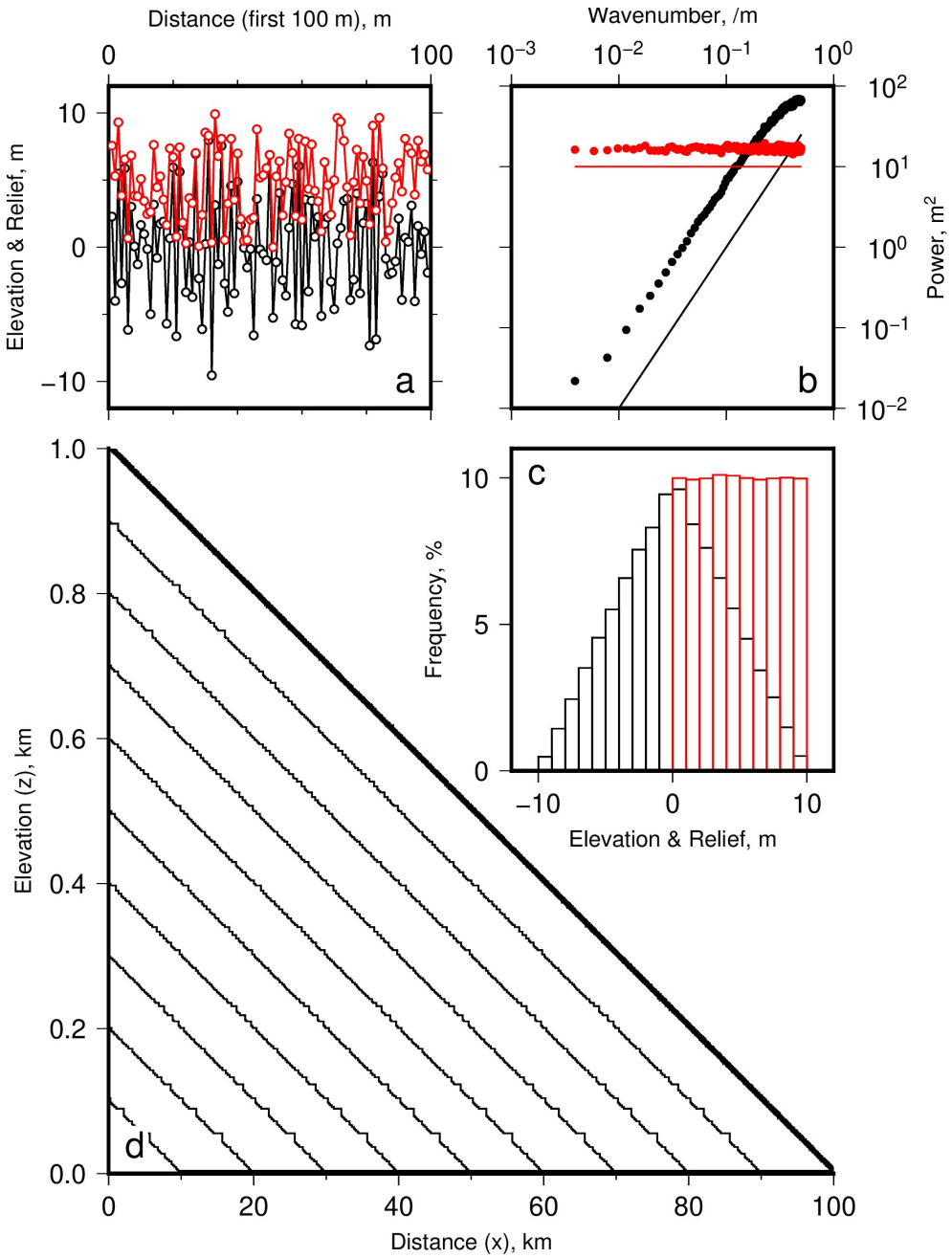

Figure 2: **Example of a 'large' model run.** (a) Red = Random uniformly distributed elevations, $z(x)$, added to the the linear slope shown in panel (d) to generate the starting condition, note that only first 100 m are shown for clarity. Black = local relief, i.e. $\Delta z = z_t^x - z_t^{x-1}$. (b) Power spectrum (from Fast Fourier Transform) of elevation (red circles) used to generate the random noise in the starting condition and relief (black circles). Note elevation spatial series has a white noise spectrum (solid red line), consistent with short wavelength ($\lesssim 100$ km) spectra of some real rivers (Roberts et al. 2019; Wapenhans et al., 2021). Black solid line = power $\propto k^2$, where k is wavenumber. (c) Histogram showing distributions of elevations (red) and relief in the starting condition (black). (d) 100-km-long river profile, containing 10^5 (1 m wide) blocks, evolving for 10^5 time steps. Thick black line = starting condition, thin lines = predicted profile every 10^4 time steps. Threshold, $c = 0.5$ m in this example. If block toppling occurs at a rate of 1 /year to 1 /century this model represents 10^5 to 10^7 years of evolution.

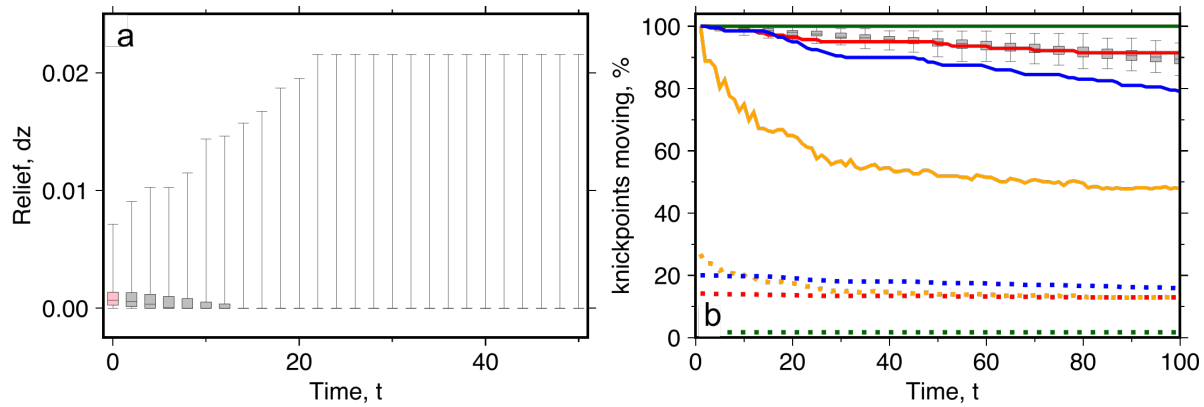

Figure 3: **Changing critical threshold, c, values.** (a) Distribution of relief as a function of time for simple linear model shown in Figure 1d–i of main manuscript; box and whiskers show extrema, median, 1st and 3rd quartile. Pink = distribution at first time step. (b) Solid curves shows percentage of knickpoints moving as a function of time relative to the number of knickpoints moving at first time step. Curves show results for different distributions of c; gray box and whiskers show distribution of values for constant value of c and 100 random distributions of starting condition (panel a and Figure 1d-i in main Ms); green/red = results for high/low constant value of c; blue = $c \propto 1/x$; orange = results for random uniform distribution of $c(x,t)$. Dotted curves = number of knickpoints moving as percentage of all relief measurements.